

PAPER • OPEN ACCESS

Mathematical modeling of radiant heat transfer in the melting furnace working space

To cite this article: V S Shvydkii *et al* 2020 *IOP Conf. Ser.: Mater. Sci. Eng.* **866** 012041

View the [article online](#) for updates and enhancements.



The Electrochemical Society
Advancing solid state & electrochemical science & technology
2021 Virtual Education

Fundamentals of Electrochemistry:
Basic Theory and Kinetic Methods
Instructed by: **Dr. James Noël**
Sun, Sept 19 & Mon, Sept 20 at 12h–15h ET

Register early and save!



Mathematical modeling of radiant heat transfer in the melting furnace working space

V S Shvydkii, V V Lavrov and E A Devyatykh

Ural Federal University n.a. the first President of Russia B.N. Yeltsin, 28 Mira Street, Ekaterinburg, 620002, Russia

E-mail: v.s.shvydkiy@urfu.ru

Abstract. The paper provides mathematical modelling results of radiation flow formation in the work space of the smelting (glassmaking, open-hearth) furnace with different heating patterns and flow distribution over the surface of the bath and enclosing structures. A significant influence of the flame length upon technical and economic parameters of furnace operation was found out.

1. Introduction

For assessment of the relation between the flame length and flow density we have built a three-dimensional mathematical model of the external problem in the furnace with a liquid bath [1-3]. For solution of the mathematical model, we used the zonal method [4-5]. In zonal method problems, separate flows have different meanings and, therefore, their relation with the flame length has its own specific features [6-8]. In terms of the balance, resulting flows have the biggest relation with heat consumptions (including fuel consumption). Here, first of all, differences in zone types and heat-exchange patterns become evident. The surface of melt is a zone of class II. For these zones heat consumptions are set as values of specific resulting flows (heat losses through the basin walls and bottom are also considered). For this reason, the flame length has an impact only on local heat-exchange characteristics – at average, the situation shall not depend on the flame length.

2. Density of Thermal Flows on the Surface of Melt and Furnace Roof

Table 1 presents data confirming this statement. The figures in the last column of table 1 characterize the spread in values of resulting flows (their root-mean-square deviation). It is determined by the formula:

$$\sigma_q = \sqrt{\frac{1}{L \cdot B} \int_0^L \int_0^B [q(x, y) - q_{mean}]^2 dx dy},$$

where L is a furnace length, m and B is a furnace width, m.

Table 1. Parameters of resulting flows on the surface of glass melt.

Flame Length, m	q_{max} , kW	x_{max} , m	y_{max} , m	Q_{mean} , kW	σ_q , kW
3.178	1906.513	6.339	1.773	546.624	441.634
6.300	1913.720	6.350	1.722	548.651	442.946



9.534	1917.190	6.347	1.723	548.945	443.322
11.580	1918.799	6.349	1.723	548.945	443.322
13.620	1916.399	6.349	1.727	547.699	442.840

Figure 1 shows a typical pattern of flow distribution over the surface of melt (in all figures the numbers on the curves are flow values, kW).

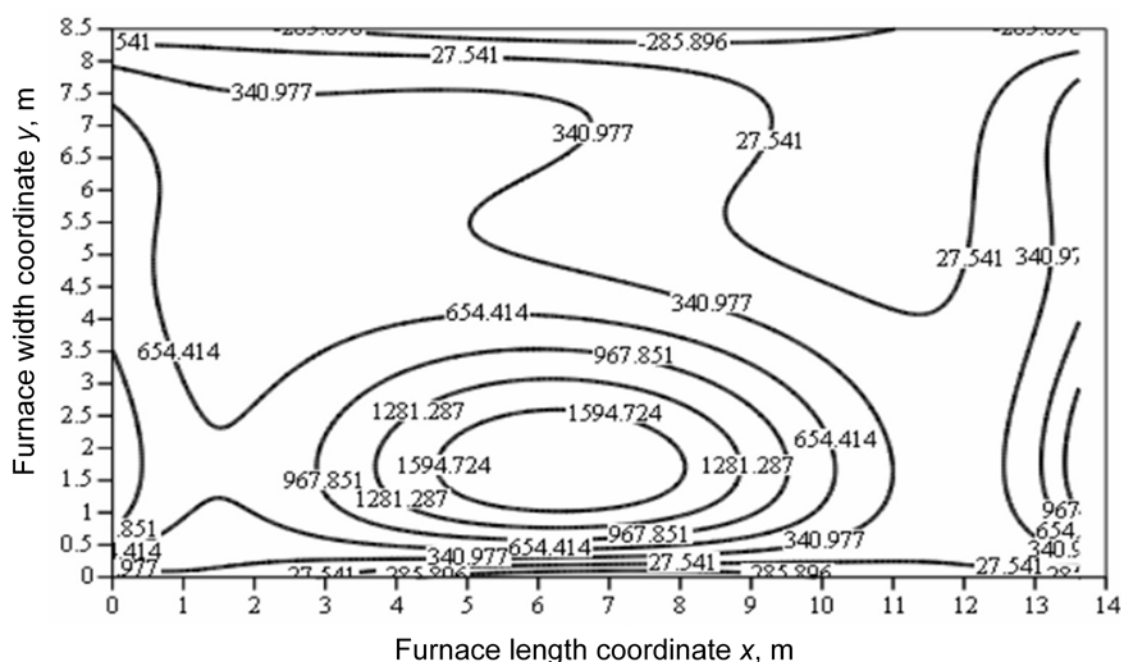


Figure 1. Resulting flows on the bath surface.

The zones of the furnace roof refer to zones of class III. For these zones, the relation between the zone temperature and resulting flow density is set. When the flame length changes, distribution of heat liberations also changes, i.e. the pattern of resulting flows depends on the flame length. The resulting flows reflect the summary total of radiant and convective heat exchange and, therefore, this dependence will not be too high but detectable anyway.

Table 2 shows parameters of resulting flow distribution over the surface of the furnace roof. As it can be seen from the data of Table 2, generally, when the flame length increases, the conditions for operation of roof refractory are getting worse as the flow values grow both at the maximum point and in the mean.

The pattern of resulting flow distribution on the furnace roof is quite typical and differs only in details at different flame length. Figure 2 shows flow distribution for a basic flame length (9.534 m) as an example.

Table 2. Parameters of resulting flows on the surface of the furnace roof .

Flame length, m	q_{max} , kW	x_{max} , m	y_{max} , m	$q_{сред}$, kW	σ_q , kW
3.178	13.266	6.087	6.758	6.936	3.277
6.300	13.624	6.563	6.529	7.613	2.997
9.534	12.998	6.985	6.236	7.997	2.827
11.58	13.466	7.202	6.268	8.395	3.020
13.62	14.089	7.113	6.313	8.412	3.093

Unlike the resulting flows that implicitly allow for heat consumptions, the incident heat flows in terms of the balance are “a half-finished product” as they characterize the heat input without tracing its further use. In this case, the difference between the glass melt surface and furnace roof surface as radiation detectors is shown only through radiative characteristics and distance to heat liberation (to the flame). As the flame is geometrically closer to the bath surface, the value of the incident flows on the bath will be somewhat higher, which is clearly seen from the comparison of the data given in table 3 and table 4.

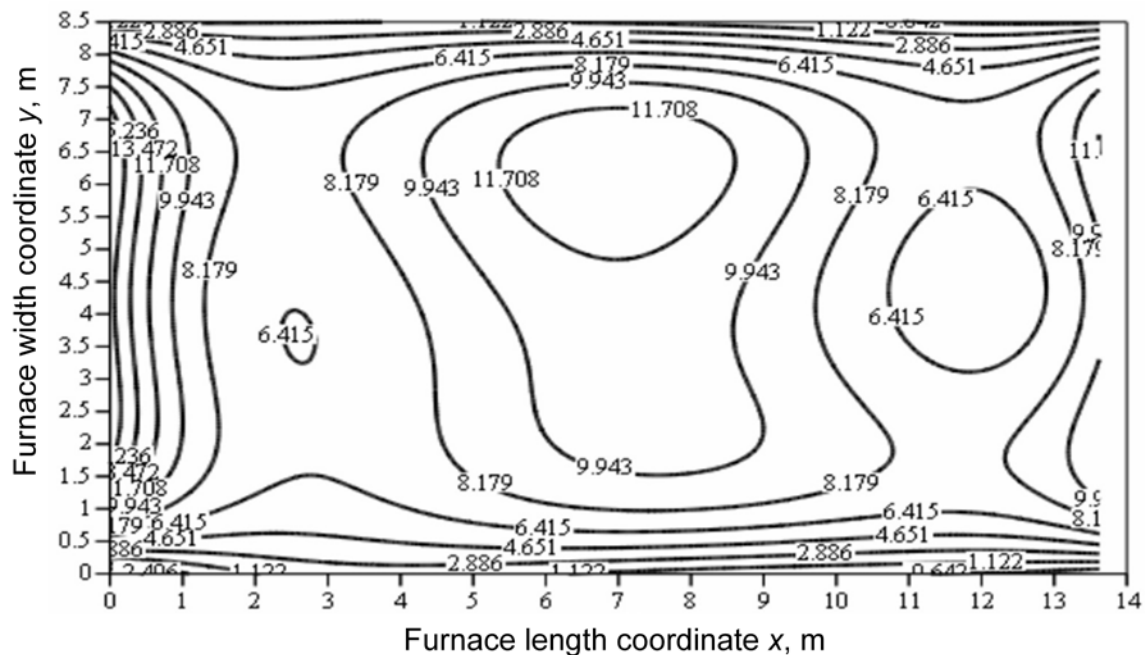


Figure 2. Distribution of resulting heat flows over the surface of the furnace roof at the basic flame length.

As it can be seen, in both cases the shortest flame (3.178 m) is out of approximately the same patterns. Flow distribution for this flame is shown in figure 3.

It shall be noted that distribution of incident flows over the surface of glass melt at this flame length is the same and there are only quantitative differences in the flows, which is already seen from the data in table 3 and table 4.

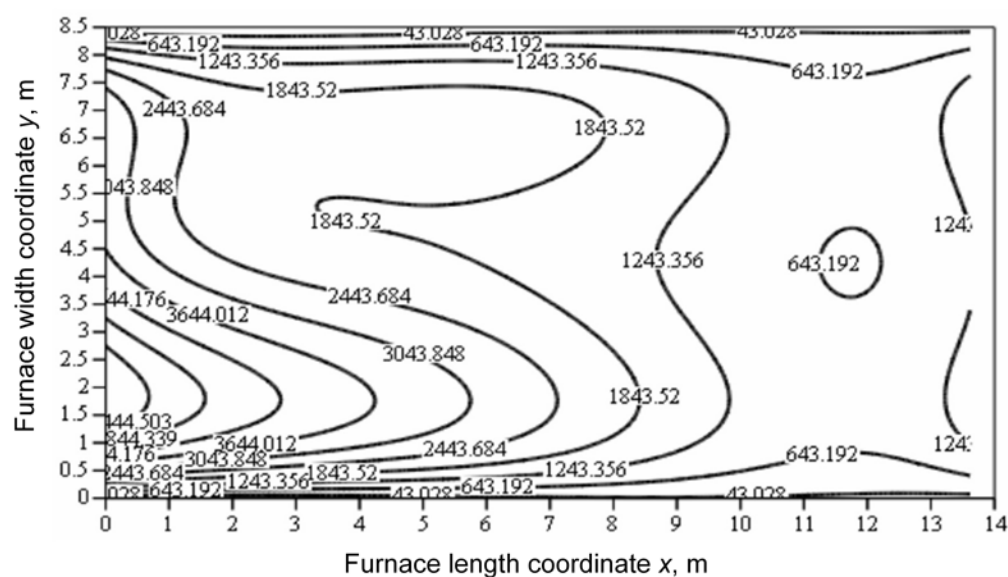
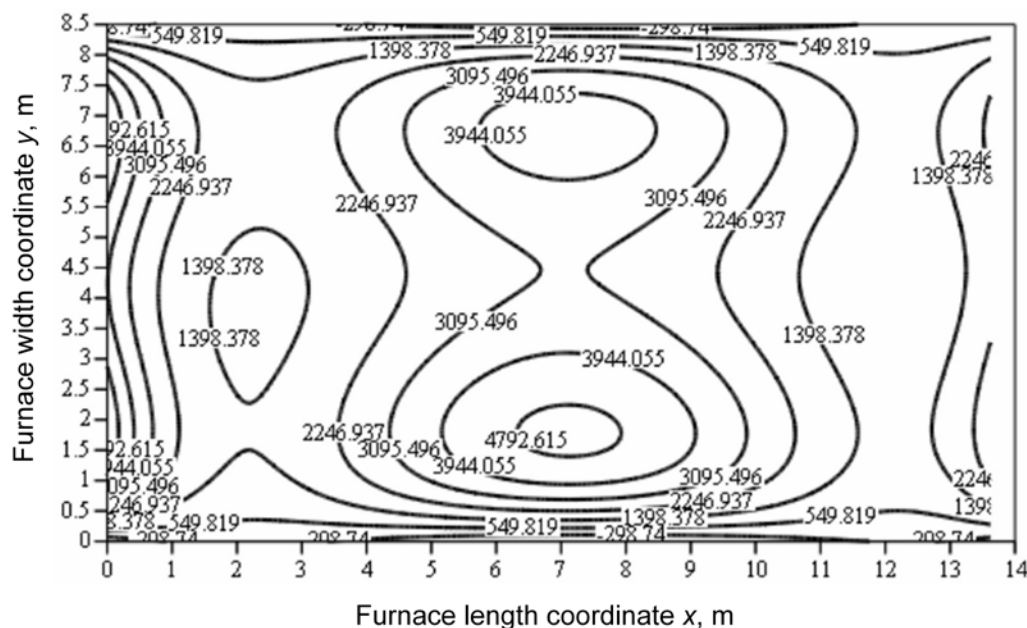
At any other flame length, distribution of incident flows both over the glass melt surface and furnace roof surface is of the same type in qualitative terms. An example of this distribution is shown in Fig.4 for the bath surface at the flame length of 11.58 m.

Table 3. Parameters of incident flows on the surface of glass melt.

Flame length, m	q_{max} , kW	x_{max} , m	y_{max} , m	q_{mean} , kW	σ_q , kW
3.178	5622.650	0.000	1.932	1817.145	1267.785
6.300	4976.533	5.655	1.792	2119.416	1221.137
9.534	5205.960	6.854	1.780	2191.285	1197.814
11.580	4975.711	7.123	1.856	2231.086	1199.315
13.620	4485.394	7.098	6.764	2125.690	1165.064

Table 4. Parameters of incident flows on the surface of the furnace roof.

Flame length, m	q_{max} , kW	x_{max} , m	y_{max} , m	q_{mean} , kW	σ_q , kW
3.178	6045.190	0.000	1.860	1774.035	1126.632
6.300	4316.125	5.335	1.786	2112.410	965.099
9.534	4424.280	6.818	1.777	2228.115	937.690
11.580	4250.628	7.169	1.842	2288.739	971.194
13.620	4035.914	7.263	6.710	2179.024	962.680

**Figure 3.** Distribution of incident flows over the surface of the furnace roof (at the flame length of 3.178 m).**Figure 4.** Distribution of incident flows over the bath surface at the flame length of 11.58 m.

3. Conclusion

Mathematic modelling of this type based on calculations within the zonal method of solution of integrodifferential equations for radiative and convective energy transfer enables to make a right choice of refractory materials for enclosing the furnace as well as optimize design and operating parameters of the furnace.

References

- [1] Shvydkii V S and Dzyuzer V Ya 2009 *Designing of Energy-efficient Glassmaking Furnaces* (Moscow: Teplotekhnika) p 339
- [2] Dzyuzer V Ya and Shvydkii V S 2016 *Refractories and Industrial Ceramics* **56(6)** 597–600
- [3] Dzyuzer V Ya, Shvydkii V S and Sadykov E B 2013 *Glass and Ceramics* **69(9-10)** 302–305
- [4] Shvydkii V S et al 1999 *The Elements of the System Theory and Numerical Methods for Modelling Processes of Heat and Mass Transfer: College Textbook* (Moscow: Intermet-Engineering) p 520
- [5] Turchak L I and Plotnikov P V 2002 *The Fundamentals of Numerical Methods: College Textbook* (Moscow: Fizmatlit) p 304
- [6] Dzyuzer V Ya 2017 *Refractories and Industrial Ceramics* **58(1)** 25–28
- [7] Sokolov B A and Abakin D A 2017 *Glass and Ceramics* **74(7-8)** pp 278–281
- [8] Sborshchikov G S and Terekhova A Yu 2017 *Glass and Ceramics* **74(1-2)** 18–19